

# Synthesis and characterization of tin oxide nanoparticles via the Co-precipitation method

SIMIN TAZIKEH<sup>1\*</sup>, AMIR AKBARI<sup>2</sup>, AMIN TALEBI<sup>1</sup>, EMAD TALEBI<sup>1</sup>

<sup>1</sup>Department of Technical Faculty, Shahrood Branch, Islamic Azad University, Shahrood, Iran

<sup>2</sup>Department of Engineering Oil and Gas Petro Tadbir Pars Company, Tehran, Iran

The present study illustrates the characteristics and co-precipitation method for synthesis of tin oxide nanoparticles. The tin oxide nanoparticles were produced using tin chloride, Triton X-100 and ammonia precipitators. Structure, size and surface morphology of the tin oxide was studied by X-ray diffraction (XRD), Fourier transform infrared spectroscopy (FTIR) and scanning electron microscopy (SEM). The results show sphere shaped tin oxide nanoparticles without chlorine contamination. The crystallite size determined by the Scherrer formula is about 23 nm. Lattice parameters calculated by Nelson-Riley equation show high quality of crystallization.

Keywords: *co-precipitation; tin oxide; nanoparticles; Nelson-Riley*

© Wroclaw University of Technology.

## 1. Introduction

Tin oxide is one of the most important materials [1] due to its high degree of transparency in the visible spectrum, strong physical and chemical interaction with adsorbed species, low operating temperature and strong thermal stability in air (up to 500 °C) [2]. Tin presents two oxidation states +2 and +4, therefore two types of oxides are possible: stannous oxide (SnO – romarchite) and stannic oxide (SnO<sub>2</sub> – cassiterite) [3], of which SnO<sub>2</sub> is more stable than SnO. SnO<sub>2</sub> is a n-type semiconductor with a wide direct band gap (3.6 eV at 300 K) [4]. It is widely used in optoelectronic devices [5], electrodes for lithium ion batteries [6], solar cells [7], transistors and gas sensors to detect the combustible gases such as H<sub>2</sub>S, CO, liquid petroleum, NO, NO<sub>2</sub> and C<sub>2</sub>H<sub>5</sub>OH [8–11]. Tin oxide nanoparticles are suitable for gas sensing applications due to high surface to volume ratio, compared to bulk tin oxide, which results in increased sensitivity and adsorption. Tin oxide nanoparticles have been prepared by physical and chemical methods. Chemical methods offer the advantage of being inexpensive and easy to per-

form. Solvents play an important role in the synthesis of tin oxide nanoparticles by chemical methods. Ethanol has been used as a solvent in this study. Ethanol is an important amphoteric solvent; it may behave as a weak acid or a weak base in different experimental conditions.

Kim et al. [12] reported thermal evaporation method for synthesis of tin oxide nanoparticles. They used pure Sn powders as a raw material and the mean size of obtained nanoparticles was 0.2 to 1.3 μm. Im et al. [13] reported using argon plasma jet for tin oxide nanoparticles synthesis. They used SnCl<sub>4</sub> and O<sub>2</sub> as raw materials an Ar as carrier gas and studied the effect of reaction gas (O<sub>2</sub>) and carrier gas (Ar) on quality of the synthesis.

Inexpensive methods for obtaining nanoparticles in low temperatures with no need of special atmosphere are the most important aims in synthesis of high quality nanoparticles. Co-precipitation is a suitable chemical method in nanoparticles synthesis because it does not require high pressure and temperature and impure materials are eliminated by filtration and washing. In present study tin oxide nanoparticles were synthesized by co-precipitation method and ultrasonic waves irradiation was used to homogenize nanoparticles.

\*E-mail: Stazikeh@yahoo.com

## 2. Experimental procedure

### 2.1. Materials

Tin chloride ( $\text{SnCl}_4$ , Merck 99 %) as starting material, Triton X-100 as surfactant, absolute ethanol as solvent, ammonia as precipitator were used to prepare tin oxide nanoparticles.

### 2.2. Preparation of tin oxide nanoparticles

$3.47 \text{ cm}^3$   $\text{SnCl}_4$  was dissolved in  $200 \text{ cm}^3$  ethanol, 5 mmol Triton X-100 was added to the solution and stirred for 30 min till a transparent solution was obtained. The ammonia solution ( $\text{NH}_4\text{OH}$ ) was dropped to the starting solution under stirring to keep a constant pH value ( $\text{pH} = 8$ ). The solution was put under an ultrasonic wave apparatus for 30 min to obtain homogenous solution which was then aged for 12 h. The precipitate was collected by filtration then washed by distilled water and ethanol for three times. After drying at  $85^\circ\text{C}$  for 4 h in oven, the precursor was calcined at  $600^\circ\text{C}$  for 1 h. After cooling, tin oxide nanoparticles were obtained.

### 2.3. Characterization

The X-ray diffraction (XRD) pattern of tin oxide nanoparticles was recorded by the D8 Advance Bruker system using  $\text{CuK}\alpha$  radiation ( $\lambda = 0.154056 \text{ nm}$ ). Particles morphology and size were investigated by scanning electron microscopy (Cam Scan MV2300). FTIR spectra of the samples were recorded with a Bruker Vector 22 equipped with a Specac Golden Gate TM ATR device working in a spectral range of  $4000 - 400 \text{ cm}^{-1}$ . The pellets were made of a mixture of 200 mg KBr dried at  $120^\circ\text{C}$  and 3 mg of the studied sample.

## 3. Result and discussion

Fig. 1 shows an XRD pattern of tin oxide nanoparticles synthesized by co-precipitation method. All of the peaks were matched with diffraction data of the tetragonal structure of tin oxide (JCPDS 00-072-1147) and no tin hydroxide peaks were observed. Position of the main peak is  $2\theta = 26.67$  and the width of the peak is  $0.36 \text{ nm}$ .

The mean crystallite size ( $D$ ) of the nanoparticles was estimated using the Debye-Scherrer formula as follows:

$$D = \frac{0.9\lambda}{\beta \cos \theta} \quad (1)$$

where  $\lambda$ ,  $\beta$ ,  $\theta$  are the X-ray wavelength of radiation used ( $\text{K}\alpha(\text{Cu}) = 0.154056 \text{ nm}$ ), the full width at half maximum (FWHM) of diffraction peak and the Bragg diffraction angle, respectively. The crystallite size ( $D$ ) determined from  $\text{SnO}_2$  (110) plane by the Scherrer formula is about  $23 \text{ nm}$ .

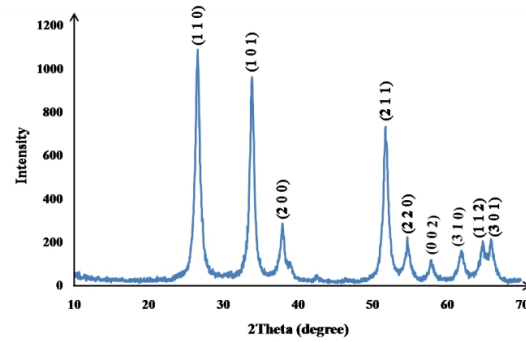


Fig. 1. XRD pattern of tin oxide nanoparticles synthesized by co-precipitation method.

The spacing between diffracting planes ( $d$ ) of  $\text{SnO}_2$  was calculated from the Bragg equation:

$$2d \cdot \sin \theta = n\lambda \quad (2)$$

and the tetragonal lattice parameter ( $a = b \neq c$ ) for the tetragonal phase structure was determined by the equation 3:

$$\frac{1}{d} = \frac{h^2 + k^2}{a^2} + \frac{l^2}{c^2} \quad (3)$$

The corrected values of lattice parameters were estimated from the Nelson-Riley [14] plots (Fig. 2). The Nelson-Riley curve was plotted between the calculated lattice parameters for different planes and error function:

$$f(\theta) = \frac{1}{2} \left( \frac{\cos^2 \theta}{\sin \theta} + \frac{\cos^2 \theta}{\theta} \right) \quad (4)$$

by the extrapolation  $f(\theta)$  vs. lattice parameter,  $a$  and  $c$  was obtained.

Lattice parameters calculated by Nelson-Riley equation are: 0.492 nm and 0.328 nm for  $a$  and  $c$ , respectively. They are in good agreement with the parameters of samples reported by other researchers and show high quality of crystallization.

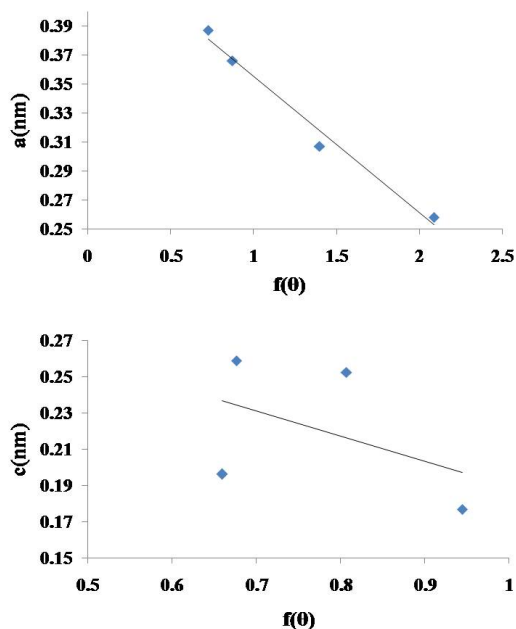


Fig. 2. Nelson-Riley plot of lattice parameters for tin oxide nanoparticles synthesized by co-precipitation method.

Fig. 3 shows SEM images of tin oxide nanoparticles synthesized by co-precipitation method. The nanoparticles have spherical morphologies with the sizes smaller than 100 nm. Slow dropping of ammonia to the solution under stirring, high-speed diffusion of ammonia in the solution and reaction happening in a large area resulted in many initial nucleases formation. Jiang et al. [15] reported that with increasing pH from 6 to 9, the particles size of tin decreased but then it did not change. So, decreasing of mean particles size with increasing pH to 9 is expected.

Fig. 4 shows the FTIR spectra of  $\text{SnO}_2$  synthesized by co-precipitation method. The band around  $3394 - 3409 \text{ cm}^{-1}$  region is due to the stretching vibration of O-H bond. This band is due to the OH groups and the adsorbed water bound

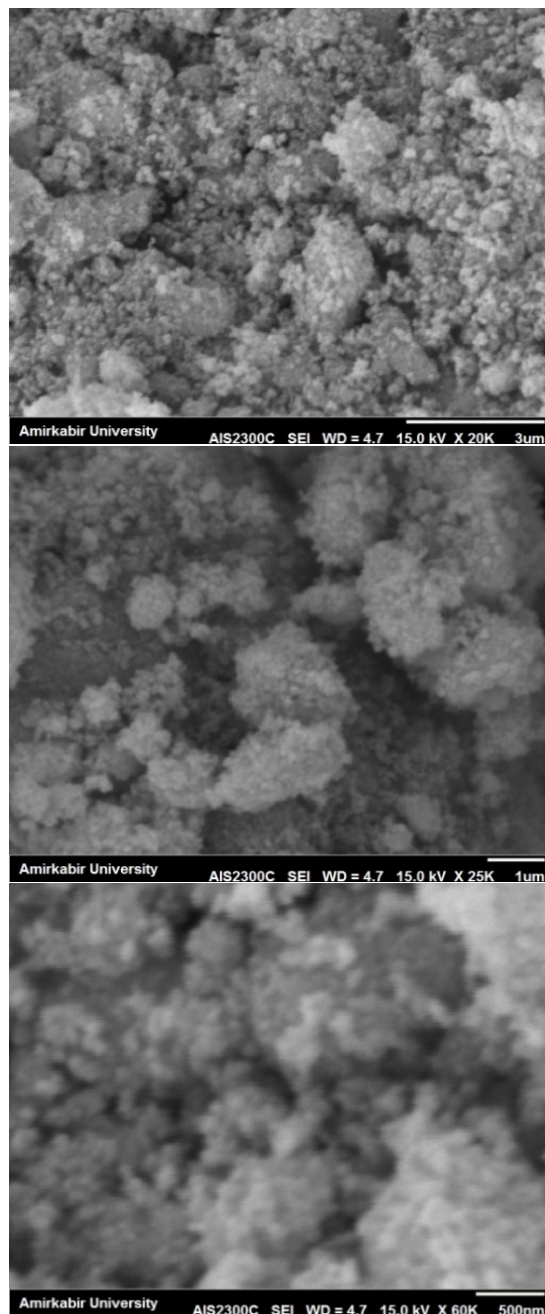


Fig. 3. The SEM images of tin oxide nanoparticles synthesized by co-precipitation method.

at the  $\text{SnO}_2$  surface. The broad band at  $1620 - 1630 \text{ cm}^{-1}$  is attributed to the bending vibration of water molecules, trapped in the  $\text{SnO}_2$  sample. The peak at  $521 \text{ cm}^{-1}$  agrees with the stretching vibrations of the terminal Sn-OH, while the peak at  $660 - 600 \text{ cm}^{-1}$  region corresponds to the stretch-

ing modes of the Sn–O–Sn. Yang et. al. [16] reported that this peak became broadened with increasing the calcination temperature.

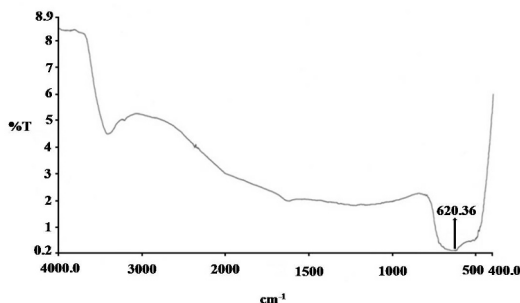


Fig. 4. FTIR spectra of tin oxide nanoparticles synthesized by co-precipitation method.

## 4. Conclusions

Tin oxide nanoparticles have been synthesized using co-precipitation method. The nanoparticles were synthesized without any requirements of special atmosphere and high pressure. FTIR studies showed that chlorine contamination was completely removed by the washing process. The tin oxide nanoparticles were finely crystallized as a tetragonal structure with spherical morphology. Lattice parameters calculated by Nelson-Riley equation showed high quality of crystallization. The present study provides inexpensive and easy method to improve the quality of tin oxide nanoparticles.

## References

- [1] GE J.P., WANG J., ZHANG H.X., WANG X., PENG Q., LI Y.D., *Sensor Actuat. B-Chem.*, 113 (2006), 937.
- [2] ADNAN R., RAZANA N.A., RAHMAN I.A., FARRUKH M.A., *J. Chin. Chem. Soc.-TAIP*, 57 (2010), 222.
- [3] VILA H.A., RODRIGUEZ-PAEZ J.E., *J. Non-Cryst. Solids*, 355 (2009), 855.
- [4] MAN L., ZHANG J., WANG J., XU H., CAO B., *Particuology*, 11 (2013), 242.
- [5] HE J.H., WU T.H., HSIN C.L., LI K.M., CHEN L.J., CHUEH Y.L., *Small*, 2 (2006), 116.
- [6] HE Z.Q., LI X.H., XION L.Z., WU X.M., XIAO Z.B., MA M.Y., *Mater. Res. Bull.*, 40 (2005), 861.
- [7] EL KHAKANI M.A., DOLBEC R., SERVENTI A.M., HORRILLO M.C., TRUDEAU M., SAINT-JACQUES R.G., RICKERBY D.G., SAYAGO I., *Sensor. Actuat. B-Chem.*, 77 (1–2) (2001), 383.
- [8] HWANG I.S., CHOI J.K., *Sensor. Actuat. B-Chem.*, 142 (2009), 105.
- [9] MOON C.S., KIM H.R., AUCHTERLONIE G., *Sensor. Actuat. B-Chem.*, 131 (2008), 556.
- [10] ZHANG J., WANG S., *Sensor. Actuat. B-Chem.*, 135 (2009), 610.
- [11] KIM K.W., CHO P.S., KIM S.J., *Sensor. Actuat. B-Chem.*, 123 (2007), 318.
- [12] KIM H.W., SHIM S.H., LEE C., *Ceram. Int.*, 32 (2006), 943.
- [13] IM J.H., LEE J.H., PARK D.W., *Surf. Coat. Tech.*, 202 (2008), 5471.
- [14] TIGAU N., CIUPINAB V., PRODANB G., RUSUC G.I., VASILE E., *J. Cryst. Growth*, 269 (2004), 392.
- [15] JIANG L., SUN G., ZHOU Z., SUN S., WANG Q., YAN S., LI H., TIAN J., GUO J., ZHOU B., XIN Q., *J. Phys. Chem. B*, 109 (2005), 8774.
- [16] YANG H., HU Y., TANG A., JIN S., QIU G., *J. Alloy. Compd.*, 363 (2004), 271.

Received 2013-09-05

Accepted 2014-01-15